

# Wave-driven Transport of Surface Oil

Rodney J. Sobey and Christopher H. Barker

Department of Civil and Environmental Engineering  
University of California, Berkeley, CA 94720, U.S.A.

## ABSTRACT

SOBEY, R.J. and BARKER, C.H., 1997. Wave-driven transport of surface oil. *Journal of Coastal Research*, 13(2), 490-496. Fort Lauderdale (Florida), ISSN 0749-0208.



The potential of surface gravity waves to transport a surface oil spill in coastal waters is investigated. A small wave-averaged surface current, directed with the waves toward the shore, is demonstrated. Wave-driven transport provides a natural mechanism for damaging beaching of surface oil. Theoretical predictions of wave-averaged surface drift are established from nonlinear steady wave theory, and an adaptation to real sea states in nearshore regions is suggested. Coupled Eulerian transport and spectral wave models provide illustrations of spill response scenarios in the nearshore wave environment.

**ADDITIONAL INDEX WORDS:** *Surface oil spill, coastal currents, Eulerian transport, nearshore waves, coastal pollution.*

## INTRODUCTION

Recent oil tanker spills (the *Exxon Valdez*, March 1989, in Prince William Sound, Alaska; the *American Trader*, February 1990, off Los Angeles, California; the *Braer*, January 1992, in the Shetland Islands) have demonstrated the particular susceptibility of the coastal environment to oil spills. Fringing beaches and coastal wetlands are especially at risk.

Existing practice in the hydrodynamic transport of surface oil slicks does not recognize the full potential of wave-driven transport. Common practice identifies tidal residual currents and wind drift as the major advective transport mechanisms, yet surface wave drift velocities can be of comparable magnitude. Significantly, this surface wave drift is directed toward the adjacent shoreline by natural refraction processes, unlike tidal, shelf and oceanographic circulations that tend to parallel the shoreline. Mass transport in these waves is concentrated in the trough-crest regions and provides a mechanism for transport of the surface slick toward the shore.

The utility of transport models depends crucially on the inclusion of those physical processes that dominate the movement of the oil slick. Wave-driven transport is often ignored, yet it may be the dominant mechanism transporting oil to adjacent beaches and coastal wetlands. Where it is claimed that wave-driven transport is considered, the surface transport has often been overlooked. Attention has been directed to longshore and undertow currents, both of which drive a transport of oil that has been mixed deeper into the water column by breaking waves. These mechanisms contribute only a very small part of the total potential for wave-driven transport.

This paper presents predictions for the wave-driven transport of a surface slick. The oil slick will impact only the ripple scales in the background wave field, and its influence on the

dominant wave numbers and frequencies has been ignored. The wave-averaged Eulerian surface drift current is predicted from nonlinear steady wave theory. An application to real sea states demonstrates the potential of the surface wave drift, compared with tidal currents and wind drift, in transporting surface oil in coastal regions.

## Eulerian Surface Drift

The literature has surprisingly little to say on the topic of wave-driven surface oil slicks. An early review (STOLZENBACH *et al.*, 1977) of oil spill transport modeling includes wave driven transport among potential advection mechanisms. Their discussion of wave-induced advection (mass transport) adopts a Lagrangian framework, focusing on the analyses of Stokes (1847; see STOKES, 1880) and LONGUET-HIGGINS (1953) for the vertical profile of the Lagrangian velocity beneath waves. Current advection (driven by tides, shelf waves and oceanic circulation) and the vertical profiles of the current are discussed in the familiar Eulerian framework. Eulerian current profiles and Lagrangian wave-induced current profiles are not comparable (Figure 1). The wave-averaged Eulerian current in a progressive wave is concentrated in the trough to crest region, whereas the wave-averaged Lagrangian current is distributed throughout the depth. Given that most measurement and modeling activities for the larger scale tidal, shelf and oceanic circulation are conducted in an Eulerian framework, present attention will be directed to the Eulerian wave-induced current, not the Lagrangian current. Stolzenbach *et al.*'s conclusion, that no adequate analytical model exists for (even the Lagrangian) oil slick advection by waves, is nonetheless notable.

Eulerian analyses of mass transport have often focused on the wave-averaged mass flux  $I$  per unit length of crest in steady progressive waves. This is a common integral parameter computed from steady wave theories. Using linear wave theory, it is approximately  $\varepsilon/C$ , where  $\varepsilon$  is the wave-averaged

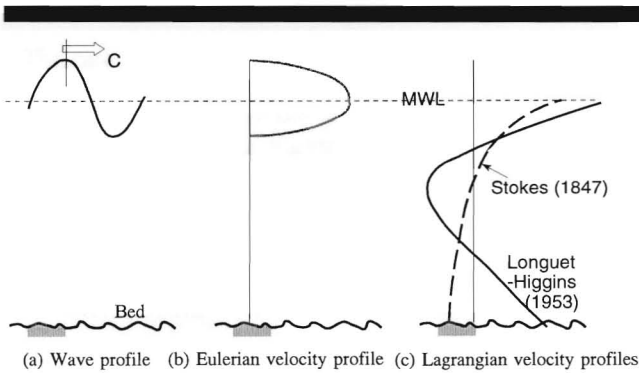


Figure 1. Eulerian and Lagrangian wave-averaged velocity profiles.

energy and  $C$  is the phase speed.  $\varepsilon$  and therefore  $I$  are second order in the wave height. The Eulerian mass flux will be small in comparison with the phase speed  $C$ , but it is always finite and positive. Unlike the wave-averaged Lagrangian mass transport that is distributed over the depth, this wave-averaged Eulerian mass transport is concentrated between the trough and the crest.

A first approximation to the Eulerian surface wave drift  $W$  can be established from the inviscid linear estimate of the wave-averaged mass flux  $I$ . Assuming the mass flux is uniformly distributed between the trough and the crest, it follows that

$$W = \frac{gH}{8C} \quad (1)$$

where  $H$  is the local wave height and  $g$  the gravitational acceleration. For a wave height  $H = 2$  m, a wave period  $T = 10$  sec and a water depth  $h = 10$  m, Equation 1 predicts an Eulerian surface drift of 0.26 m/sec.

In the absence of ambient current, existing oil slick transport models consistently assume that wind is the dominant advection mechanism. The surface wind drift is of order  $0.03U_{10}$  (the "3% rule"), where  $U_{10}$  is the wind speed at standard anemometer height. That same wind will generate waves, whose order of magnitude may be estimated from the O'Brien-Sverdrup-Munk fetch graph (e.g., WILSON, 1963) in which wave generation is represented as

$$\frac{gH_s}{U_{10}^2} = f_1 \left( \frac{gx_F}{U_{10}^2}, \frac{gt_D}{U_{10}} \right), \quad \frac{C}{U_{10}} = f_2 \left( \frac{gx_F}{U_{10}^2}, \frac{gt_D}{U_{10}} \right) \quad (2)$$

in which  $H_s$  is the significant wave height, and  $x_F$  is the fetch length and  $t_D$  the duration of the sustained wind. Assigning  $H$  in Equation 1 as the mean wave height, which is  $0.63H_s$  from the Rayleigh distribution, and then substituting Equation 2 into Equation 1 and rearranging gives the following estimate of Eulerian surface wave drift

$$W = \frac{0.63f_1}{8f_2} U_{10} \approx 0.015U_{10} \quad (3)$$

where the approximate result corresponds to a  $f_1/f_2$  ratio appropriate to a moderate sea state.

Typical estimators of both wind drift and wave drift are

similar in magnitude. There is a clear indication that surface wave drift can be an important contributor to net advection of surface oil slicks. This seems to be implicitly recognized in recent practice by the adjustment of the "3% rule" to a "4 or 5% rule" to accommodate combined wind and wave drift. Later reviews (e.g., SPAULDING, 1988) of the simulation of oil spill transport list potential advection mechanisms as wind, current, and waves. Nonetheless, waves have consistently been viewed as a minor influence, the dominant advection mechanisms being wind and (tidal and oceanographic) currents.

While Equation 3 clearly demonstrates that an increase in the magnitude of the wind drift reasonably accommodates the influence of wave drift, this approach remains appropriate only while the waves are directly related to the local wind and continue to propagate in essentially the same direction as the local wind. This describes the local wind sea, and then only while refraction influences are negligible. Incident swell waves cannot be accommodated in this manner. They are unrelated to the local wind in both magnitude and direction. Advection directions in particular are unlikely to correspond. Significantly, nearshore refraction directs both swell waves and local wind seas to the fringing shoreline, whereas ambient currents are directed parallel to the fringing shoreline.

Some attempt is made to include wave driven transport in more recent oil spill models for the nearshore zone by BORTHWICK and JOYNES (1989) and REED *et al.* (1989). Unfortunately, their interpretation of wave-driven transport is not complete. They ignore the surface drift and include only a very small part of the potential transport. BORTHWICK and JOYNES (1989) equate wave-driven oil slick transport in the nearshore region to advection by the horizontal circulation (longshore current and undertow in the surf zone, rip currents and return flow seaward from the breakers) driven by the wave field. REED *et al.* (1989) further restrict this interpretation to advection by the longshore current within the surf zone. While a complete horizontal circulation pattern of longshore current, undertow, rip currents and broad return flow will certainly exist and is indeed wave-driven (BATTJES *et al.*, 1990), these currents exist below the wave troughs and will transport only that part of the surface oil slick that has been forced into solution deeper into the water column by breaking waves.

Both the direction and magnitude of the surface transport conflict fundamentally with the below-trough transport. In particular, neither the longshore current (directed alongshore within the surf zone) nor the undertow current (directed offshore) coincide with the local direction of wave propagation, differing in direction by approximately  $90^\circ$  and  $180^\circ$  respectively. The local wave-averaged surface wave drift  $W$  will correspond with the local wave direction. The direction of the wave-averaged horizontal Eulerian velocity will spiral with depth from a surface direction corresponding with the direction of local wave propagation to a deeply submerged depth approximating the local component of the horizontal circulation (BATTJES *et al.*, 1990). The circulation cells will move oil alongshore and back out to sea. This horizontal circulation will not move surface oil to the shore.

### THEORETICAL PREDICTIONS OF SURFACE DRIFT

Theoretical predictions of the wave-averaged Eulerian surface drift can be established under idealized conditions, namely for a steady progressive (and nonlinear) wave train. Given reliable estimates of surface kinematics, the Eulerian surface wave drift velocity at a particular position  $x$  is available as

$$W = \frac{1}{T} \int_0^T u(z = \eta, t; x) dt \tag{4}$$

where  $u$  is the horizontal water particle velocity at the water surface  $\eta(t; x)$  at time  $t$ , and  $T$  is the wave period. The surface wave drift is not the same as the mean mass transport velocity or Stokes' drift velocity,

$$U_s = \frac{1}{hT} \int_{-T/2}^{T/2} \int_{-h}^{\eta} u(z, t; x) dz dt \tag{5}$$

which is a routine integral parameter in steady wave theory.

Using Airy or linear wave theory, together with a Taylor series expansion about the MWL, to represent the near-surface kinematics, the wave-averaged surface drift becomes

$$\begin{aligned} W &= \frac{1}{T} \int_0^T a\omega \frac{\cosh k(h + \eta)}{\sinh kh} \cos(kx - \omega t) dt \\ &= \frac{a\omega}{2\pi} \int_{-\pi}^{\pi} \left[ \frac{\cos \theta}{\tanh kh} \left( 1 + \frac{1}{2}k^2\eta^2 + \dots \right) \right. \\ &\quad \left. + \cos \theta \left( k\eta + \frac{1}{3}k^3\eta^3 + \dots \right) \right] d\theta \\ &= \frac{1}{2}(ka)^2C + \dots \end{aligned} \tag{6}$$

in which  $a$  is the wave amplitude,  $\omega$  is the wave frequency,  $k$  is the wave number and  $\theta = kx - \omega t$  is the wave phase.

Like the wave-averaged mass-flux or momentum, the wave-averaged momentum flux, the wave-averaged energy and energy flux, the wave-averaged surface drift is second order in the wave height. For a wave height  $H = 2$  m, a wave period  $T = 10$  sec and a water depth  $h = 10$  m, Equation 6 predicts an Eulerian surface drift of 0.021 m/sec. This result differs by an order of magnitude from the Equation 1 prediction of 0.26 m/sec. This poor agreement suggests that linear theory may not provide an adequate estimate of the surface drift.

Theories for the prediction of kinematics within surface gravity waves are less accurate at the water surface, just where the present interest in surface wave drift is focused. The difficulties are associated with the free surface boundary conditions; the dynamic condition is nonlinear and both the kinematic and dynamic conditions are applicable along the water surface whose location is itself part of the solution sought. Different order theories are distinguished principally by the accuracy of representation of these free surface boundary conditions.

Low order theories, especially Airy or linear theory, make major assumptions at the free surface and may lead to spu-

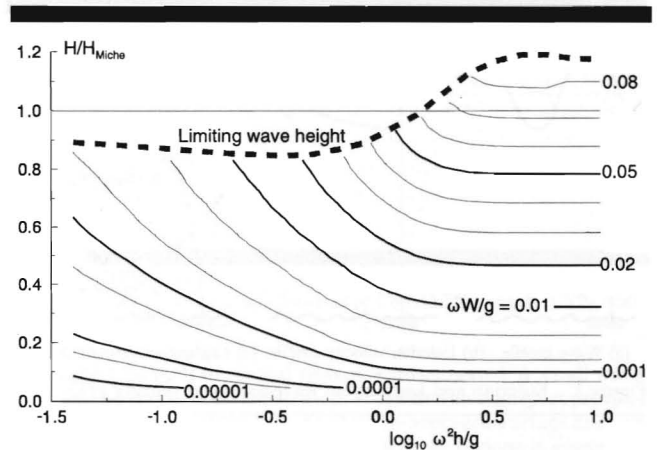


Figure 2. Steady wave theory prediction of wave-averaged surface drift.

rious predictions of the surface kinematics. The theoretical prediction of the surface wave kinematics were based on high order Fourier wave theory (e.g., SOBEY, 1989). To all pragmatic purposes, this is an exact steady wave theory, provided only (SOBEY, 1988) that appropriate attention is given to the truncation order and the number of computational nodes along the free surface. The Equation 4 integral has been evaluated numerically from predictions of horizontal velocity at closely spaced points along the predicted water surface.

The horizontal particle velocity at the water surface, and therefore the surface drift, is dependent on wave period  $T$ , wave height  $H$ , water depth  $h$  and co-flowing current  $U$ . Results have been organized in a non-dimensional framework

$$\frac{\omega W}{g} = f\left(\frac{\omega^2 H}{g}, \frac{\omega^2 h}{g}, \frac{\omega U}{g}\right) \tag{7}$$

where  $\omega = 2\pi/T$  is the wave frequency and  $g$  is the gravitational acceleration. Computations of  $\omega W/g$  have been completed for a parameter range covering the complete spectrum of dimensionless wave height and water depth that might be expected in practice; current has been ignored in the present study. To achieve adequate resolution in shallow water with this presentation, the wave height has been normalized by the Miche (1944) analytical estimate for the breaking wave height,  $H_{Miche} = 0.14L \tanh kh$ , in which  $L = 2\pi/k$  and  $k$  is the wave number predicted by linear wave theory. This result, though approximate, is useful for data presentation purposes. The results, presented as

$$\frac{\omega W}{g} = f\left(\frac{H}{H_{Miche}}, \frac{\omega^2 h}{g}\right) \tag{8}$$

are shown in Figure 2. Almost exact estimates of the theoretical limit wave height are provided by the numerical Williams (1985) tables; this provides the upper bound to the plot.

For a wave height  $H = 2$  m, a wave period  $T = 10$  sec and a water depth  $h = 10$  m, the Equation 8 predicted Eulerian surface drift is 0.031 m/sec; the linear Equation 6 prediction was 0.021 m/sec.

## SURFACE DRIFT IN A REAL SEA STATE

The calming effect of small quantities of oil on water surface waves has been known since classical times. Surface contamination can influence the shear stress at the water surface and especially the pressure that can be supported across the water surface. The impact is most influential on small capillary waves or ripples. Viscosity has a negligible effect on damping of ripples, but increasing surface tension is most effective in damping the ripples. However, there are no known surface films that could suppress surface waves longer than about 1 m in length (GOTTIFREDI and JAMESON, 1968). The dominant wave lengths of observed seas are of order 100 m. At sea, the ground swell continues but the small capillary waves disappear.

Real sea states are commonly described by the local directional variance spectrum  $E(\omega, \theta; x, y, t)$ , which will vary with horizontal position  $x, y$  and evolve with time  $t$ . In the spirit of the directional spectrum description of the sea state, a local directional spectrum description of the surface wave drift, as  $E_w(\omega, \theta; x, y, t)$ , is anticipated.  $E_w$  is defined as complex, such that the local net surface wave drift vector is

$$\begin{aligned} \bar{W}_x + i\bar{W}_y &= \int_{-\pi}^{\pi} \int_0^{\infty} E_w(\omega, \theta) d\omega d\theta \approx \sum_i \sum_j E_w(\omega_i, \theta_j) \Delta\omega_i \Delta\theta_j \end{aligned} \quad (9)$$

with magnitude and direction

$$\bar{W} = \sqrt{\bar{W}_x^2 + \bar{W}_y^2} \quad (10)$$

$$\bar{\theta} = \tan^{-1} \frac{\bar{W}_y}{\bar{W}_x} \quad (11)$$

respectively.

In each frequency-direction band of width  $\Delta\omega_i, \Delta\theta_j$  centered at  $\omega_i, \theta_j$ , the contribution to the sea state variance is  $E(\omega_i, \theta_j)\Delta\omega_i\Delta\theta_j$ . The theoretical predictions for surface wave drift have been established for steady, monochromatic and progressive waves in water of constant depth and zero current. The sea state variance for a linear, monochromatic wave of height  $H_i$  is  $H_i^2/8$ , whence

$$H_i = \sqrt{8E(\omega_i, \theta_j)\Delta\omega_i\Delta\theta_j} \quad (12)$$

and  $W(\omega_i, \theta_j)$  can be estimated by interpolation from Figure 2.  $W(\omega_i, \theta_j)[\cos \theta_j + i \sin \theta_j]$  is the contribution  $E_w(\omega_i, \theta_j)\Delta\omega_i\Delta\theta_j$  to the  $E_w(\omega, \theta)$  spectrum. Under swell conditions, there may be only a single direction-frequency band.

## TRANSPORT OF SURFACE OIL

Predictive models of flow processes in the natural environment are mostly based on the Eulerian description of the flow. Oil spill transport models have often been the exception to this otherwise universal practice. Most existing models have adopted a Lagrangian description, an exception being the NIHOUL (1984) Eulerian model. Eulerian models appear certain to be used more frequently in the future, not the least because of the increasing need to couple oil spill transport models with (Eulerian) hydrodynamic models of current circulation in estuaries, bays and nearshore regions and (Eulerian)

meteorological models of the flow in the lower atmospheric boundary layer.

The Eulerian transport equation for a surface oil slick is a mass conservation equation for the surface oil layer. It is

$$\frac{\partial C}{\partial t} + \frac{\partial}{\partial x}(u_s C) + \frac{\partial}{\partial y}(v_s C) = \frac{\partial}{\partial x}\left(E_x \frac{\partial C}{\partial x}\right) + \frac{\partial}{\partial y}\left(E_y \frac{\partial C}{\partial y}\right) + S \quad (13)$$

in which  $C = d\Delta\rho$  is the local concentration of surface oil,  $\Delta\rho$  is the local mass density deficit of oil relative to water,  $d$  is the local depth of the oil layer,  $u_s$  and  $v_s$  are the local components of the surface current,  $E_x$  and  $E_y$  are the local dispersion coefficients in the  $x$  and  $y$  directions respectively, and  $S$  is the local mass transfer rate from source/sink processes.

The initial term  $\partial C/\partial t$  in Equation 13 is the local rate of change in the concentration of surface oil. Physically, the complete equation describes how this responds to advection (terms 2 and 3), to dispersion (terms 4 and 5) and to source/sink processes (term 6).

Advection by surface currents is the dominant transport process. Wind and ambient tidal and geostrophic currents are familiar contributors, in addition to wave-driven surface currents, which are the focus of the present study. Classical shear flow dispersion has not been separated from the advective transport. However, the initial buoyant spreading (e.g., HOULT, 1972) has been shown (SOBEY, 1992) to be equivalent to a dispersive process with dispersion coefficient

$$E = \begin{cases} \frac{1}{2} \left( g \frac{\Delta\rho}{\rho_w} V \right)^{1/2} & \text{for } t \leq 1 \text{ hr} \\ \frac{1}{2} \nu^{-1/6} \left( g \frac{\Delta\rho}{\rho_w} V^2 \right)^{1/3} t^{-1/2} & \text{for } 1 \text{ hr} \leq t \leq 1 \text{ week} \end{cases} \quad (14)$$

in which  $V$  is the initial volume of surface oil,  $\nu$  is the kinematic viscosity of the surface oil,  $\rho_w$  is the mass density of sea water, and  $t$  is the time after the initial spill. Though initially constant in the immediate buoyancy-inertia regime, the dispersion coefficient decays in magnitude with time after the spill in the dominant buoyant-viscous drag regime.

Source/sink processes include beaching and weathering processes, both of which are negative source (i.e., sink) terms, extracting mass from the slick. Beaching is perhaps the major environmental concern and accounts for a major proportion of the spill volume. In the 1978 *Amoco Cadiz* spill along the Brittany coast of France, an estimated 28% came ashore (GUNDLACH *et al.*, 1983), comparable to the estimated 30% attributed to evaporation and 20.5% that could not be accounted for. The processes involved in beaching are complicated and not well understood. Weathering processes, especially evaporation but also emulsification and biodegradation, transfer mass from the water surface to the atmosphere and deeper into the water column. They contribute slowly but persistently, eventually accounting for the major part of the mass budget. Weathering influences are rarely strong in the initial few days, when transport is dominated by advection.

Numerical solutions of the Eulerian transport equations must accommodate potentially severe numerical diffusion and solution oscillation problems but suitable algorithms are

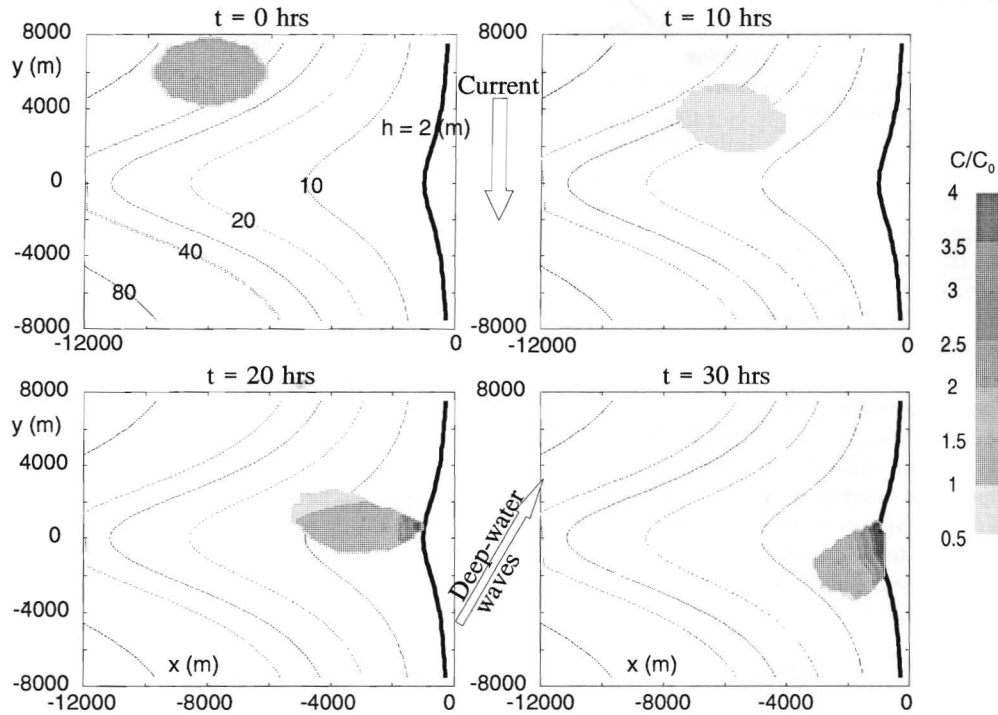


Figure 3. A simulation of wave-driven transport of surface oil.

available. Anticipating the fractional step algorithm, equation 13 is recast in operator notation as

$$\frac{\partial C}{\partial t} = (A_1 + A_2 + A_3)C \tag{15}$$

in which

$$A_1 C = -\frac{\partial}{\partial x}(u_s C) - \frac{\partial}{\partial y}(v_s C) \tag{16}$$

$$A_2 C = \frac{\partial}{\partial x}\left(E_x \frac{\partial C}{\partial x}\right) + \frac{\partial}{\partial y}\left(E_y \frac{\partial C}{\partial y}\right) \tag{17}$$

$$A_3 C = S \tag{18}$$

Operators  $A_1$  through  $A_3$  identify the three physically distinct processes influencing the transport, namely advection, dispersion and generation. Using the fractional step algorithm, each of these processes is considered separately and sequentially. As it is not necessary to impose a single solution algorithm on all processes, different algorithms, suitable for the separate steps, can be adopted (SOBEY, 1983).

Focusing attention now just on the wave-driven transport, all but the advective step is ignored. From the method of characteristics, the transport equation is exactly equivalent to the set of equations

$$\frac{dC}{dt} = -C\left(\frac{\partial u_s}{\partial x} + \frac{\partial v_s}{\partial y}\right)$$

along

$$\frac{dx}{dt} = u_s, \quad \frac{dy}{dt} = v_s \tag{19}$$

Equations 19 describe the evolution of the surface oil slick as an initial value problem. The concentration evolves along these characteristic paths in response to the divergence of the local surface current field. Given the surface velocity field, Equations 19 are a set of three simultaneous ordinary differential equations, which may be integrated numerically to excellent precision by classical Runge-Kutta algorithms. The initial distribution of the oil is described by a suitable collection of nodal points at which the oil concentration is known. These nodes need not be distributed on a uniform grid, as the distribution will soon become irregular in response to velocity shear. This numerical algorithm is almost exact (BODE and SOBEY, 1984).

### WAVE-DRIVEN TRANSPORT IN A NEARSHORE WAVE FIELD

A simulated spill in a nearshore wave field will demonstrate the potential of wave-driven transport. The offshore bathymetry and the initial location of the spill are shown in Figure 3a. The origin of coordinates is located at the shoreline intersection with a ridge feature. The spill is initially circular in shape, with uniform concentration  $C_0$  and located at (-8,000 m, 6,000 m) where the water depth is about 50 m. There is a uniform longshore current of (0-0.1 m/sec). The incident wave field in deep water is uniform with a Pierson-Moskowitz-based directional spectrum

$$E(\omega, \theta) = \frac{\alpha g^2}{\omega_p^4} \left(\frac{\omega}{\omega_p}\right)^{-5} \exp\left[-1.25\left(\frac{\omega}{\omega_p}\right)^{-4}\right] \frac{8}{3\pi} \cos^4(\theta - \theta_0) \tag{20}$$

in which  $\alpha$  is the Phillips coefficient, the peak frequency  $f_p$  is

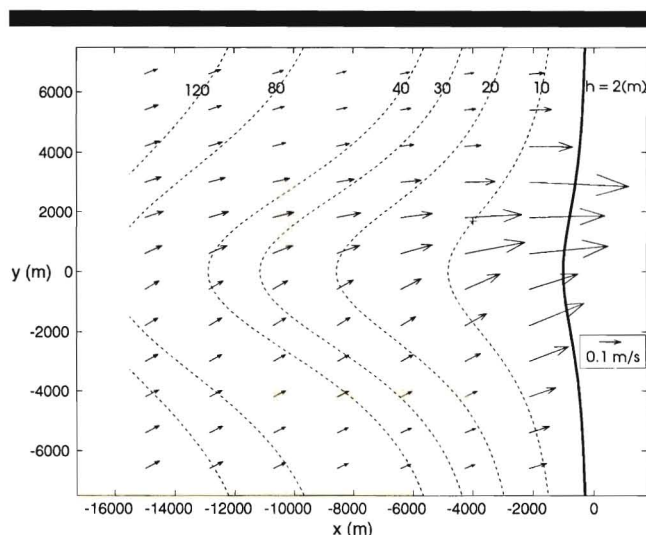


Figure 4. Dominant surface drift field.

0.10 Hz ( $\omega_p = 2\pi f_p$ ), the dominant direction  $\theta_0$  is  $60^\circ$ , and the spectral variance  $\sigma^2$  is  $1 \text{ m}^2$ , equivalent to mean and significant wave heights of 2.50 and 4.0 m respectively. This is a moderate sea state on an open coast.

The nearshore wave field has been computed from a spectral wave model (SOBEY and YOUNG, 1986) based in the radiative transfer equation. Generation and dissipation within the nearshore zone have been omitted for this illustration. Given this local prediction of the direction spectrum, the surface wave drift has been determined from Equations 10 and 11. The net local surface drift was determined from vector addition of this current with the longshore current, ignoring wave-current interaction. Figure 4 shows the vector field of the dominant surface drift, together with the bathymetric contours throughout the solution field.

Figures 3a through d shows the simulated transport of the slick over a 30 hour period, under the combined influence of waves and longshore current. A simple beaching algorithm, in which all oil is assumed to be beached on reaching the 2 m depth contour, has been adopted. Surface oil concentrations are shown on a gray scale. Without wave-driven transport in this case, the oil slick would be transported alongshore with the longshore current. It would not be beached. With wave-driven transport, beaching of oil begins about 20 hours after the spill. Refraction influences over the ridge feature initially disperse (at  $t = 10$  hours) and subsequently strongly concentrate the slick along and near the shoreline. Other simulations consistently repeat this pattern.

The present study has focussed on the less familiar aspects of wave-driven transport in coastal waters. An operational model that included wave-driven transport along with wind and current advection would need to give attention to a range of additional processes, including local wind-wave generation, wave breaking and wave-driven nearshore circulation, wave-current interaction, and especially the beaching process. Wave breaking and the associated turbulence will mix a part of the buoyant surface oil into the water column, which can

then be advected alongshore and perhaps offshore by the local current pattern. The beaching of oil in the surf zone is a very complicated process, to which little attention seems to have been given.

## CONCLUSIONS

The horizontal velocity at the water surface in progressive surface gravity waves has a net forward component in the direction of wave propagation. Though small, and second order in the wave height, this surface velocity is always directed toward fringing beaches and coastal wetlands, unlike tidal and oceanographic currents which are constrained to flow parallel to the shore. The wave-induced surface transport provides a natural mechanism for beaching of surface oil, perhaps the most damaging outcome of a coastal oil spill.

Theoretical predictions for wave-averaged surface wave drift have been established (Figure 2) from nonlinear steady wave theory for the complete range of wave height, wave period and water depth expected in practice. Adaptions of these predictions, Equations 10 and 11, have been suggested for real sea states.

The transport of surface oil can be described by an Eulerian transport equation, which identifies the causative processes of advection, dispersion (buoyant spreading) and generation (weathering and beaching). Coupled Eulerian transport and spectral wave models have been used to demonstrate (Figure 3) the potential of wave-driven transport in the nearshore wave environment. Any nearshore wave field, through natural shoaling and refraction processes, will drive a transport inexorably toward the shore.

## ACKNOWLEDGMENTS

Martha Jordan contributed to the computations on which Figure 2 is based. This paper is funded by a grant from the National Sea Grant College Program, National Oceanic and Atmospheric Administration, U.S. Department of Commerce, under grant number NA36RG0537, project number R/CZ-118 through the California Sea Grant College, and in part by the California State Resources Agency. The views expressed herein are those of the authors and do not necessarily reflect the views of NOAA or any of its sub-agencies. The U.S. Government is authorized to reproduce and distribute for governmental purposes.

## LITERATURE CITED

- BATJES, J.A.; SOBEY, R.J., and STIVE, M.J.F., 1990. Nearshore circulation. In LE MEHAUTE, B. and HANES, D.M. (eds.), *The Sea, Vol.9: Ocean Engineering Science*. New York: Wiley, 467-493.
- BODE, L. and SOBEY, R.J., 1984. Accurate modelling of two-dimensional mass transport. *Proceedings, 19th Conference on Coastal Engineering* (Houston), New York: ASCE, Vol. 3, pp. 2434-2448.
- BORTHWICK, A.G.L. and JOYNES, S.A., 1989. Horizontal dispersion of oil pollutant in coastal waters. *Proceedings, International Conference on Hydraulic and Environmental Modelling of Coastal, Estuarine and River Waters* (Bradford, U.K.), Aldershot: Gower Technical, pp. 322-331.
- GOTTIFREDI, J.C. and JAMESON, G.J., 1968. The suppression of wind-generated waves by a surface film. *Journal of Fluid Mechanics*, 32, 609-618.
- GUNDLACH, E.R.; BOEHM, P.D.; MARCHAND, M.; ATLAS, R.M.;

- WARD, D.M., and WOLFE, D.A., 1983. The fate of Amoco Cadiz oil. *Science*, 221, 122-129.
- HOULT, D.P., 1972. Oil spreading on the sea. *Annual Review of Fluid Mechanics* 4, 341-368.
- LONGUET-HIGGINS, M.S., 1953. Mass transport in water waves. *Philosophical Transactions, Royal Society, London, Series A*, 345, 535-581.
- MICHE, R., 1944. Mouvements ondulatoires de la mer en profondeur constante ou décroissante. 3me Partie. *Annales des Ponts et Chaussées*, 114, 369-406.
- NIHOUL, J.C.J., 1984. A non-linear mathematical model for the transport and spreading of oil slicks. *Ecological Modelling*, 22, 325-339.
- REED, M.; GUNDLACH, E., and KANA, T., 1989. A coastal zone oil spill model: Development and sensitivity studies. *Oil and Chemical Pollution*, 5, 411-449.
- SOBEY, R.J., 1983. A fractional step algorithm for estuarine mass transport. *International Journal for Numerical Methods in Fluids*, 3, 567-582.
- SOBEY, R.J., 1988. Truncation order of Fourier wave theory. *Proceedings 21st Conference on Coastal Engineering (Malaga)*, New York: ASCE, Vol. 1, pp. 307-321.
- SOBEY, R.J., 1989. Variations on Fourier wave theory. *International Journal for Numerical Methods in Fluids*, 9, 1453-1467.
- SOBEY, R.J., 1992. *Physical Processes in the Transport of Surface Oil Slicks*. San Francisco: Philip Williams & Associates, Ltd., 14p.
- SOBEY, R.J. and YOUNG, I.R., 1986. Hurricane wind waves—A discrete spectral model. *Journal of Waterway, Port, Coastal and Ocean Engineering*, 112, 370-389.
- SPAULDING, M.L., 1988. A state-of-the-art review of oil spill trajectory and fate modeling. *Oil and Chemical Pollution*, 4, 39-55.
- STOKES, G.G., 1880. *Mathematical and Physical Papers*, Vol. I. Cambridge: University Press.
- STOLZENBACH, K.D.; MADSEN, O.S.; ADAMS, E.E.; POLLACK, A.M., and COOPER, C.K., 1977. A review and evaluation of basic techniques for predicting the behavior of surface oil slicks. *Report 222*. Cambridge, MA: Ralph M. Parsons Laboratory, Massachusetts of Technology.
- WILLIAMS, J.M., 1985. *Tables of Progressive Gravity Waves*. Boston: Pitman.
- WILSON, B.W., 1963. Deep water wave generation by moving wind systems. *Journal of Waterways and Harbors Division, ASCE*, 87, 113-141.